Atmos. Meas. Tech., 6, 3099–3113, 2013
www.atmos-meas-tech.net/6/3099/2013/
doi:10.5194/amt-6-3099-2013

Atmospheric Measurement Techniques
Open Access

HCl and ClO profiles inside the Antarctic vortex as observed by SMILES in November 2009: comparisons with MLS and ACE-FTS instruments

T. Sugita[1], Y. Kasai[2], Y. Terao[1], S. Hayashida[3], G. L. Manney[4,5], W. H. Daffer[6], H. Sagawa[2], M. Suzuki[7], M. Shiotani[8], K. A. Walker[9,10], C. D. Boone[10], and P. F. Bernath[11,12]

[1]National Institute for Environmental Studies, Tsukuba, Ibaraki, Japan
[2]National Institute of Information and Communications Technology (NICT), Koganei, Tokyo, Japan
[3]Faculty of Science, Nara Women's University, Nara, Japan
[4]NorthWest Research Associates, Inc., Socorro, New Mexico, USA
[5]New Mexico Institute of Mining and Technology, Socorro, New Mexico, USA
[6]Jet Propulsion Laboratory, California Institute of Technology, Pasadena, California, USA
[7]Institute of Space and Astronautical Science, Japan Aerospace Exploration Agency (JAXA), Sagamihara, Kanagawa, Japan
[8]Research Institute for Sustainable Humanosphere, Kyoto University, Uji, Kyoto, Japan
[9]Department of Physics, University of Toronto, Toronto, Ontario, Canada
[10]Department of Chemistry, University of Waterloo, Waterloo, Ontario, Canada
[11]Department of Chemistry and Biochemistry, Old Dominion University, Norfolk, Virginia, USA
[12]Department of Chemistry, University of York, Heslington, York, UK

Correspondence to: T. Sugita (tsugita@nies.go.jp)

Received: 8 July 2013 – Published in Atmos. Meas. Tech. Discuss.: 23 July 2013
Revised: 15 October 2013 – Accepted: 16 October 2013 – Published: 18 November 2013

Abstract. We present vertical profiles of hydrogen chloride (HCl) and chlorine monoxide (ClO) as observed by the Superconducting Submillimeter-Wave Limb-Emission Sounder (SMILES) on the International Space Station (ISS) inside the Antarctic vortex on 19–24 November 2009. The SMILES HCl value reveals 2.8–3.1 ppbv between 450 K and 500 K levels in potential temperature (PT). The high value of HCl is highlighted since it is suggested that HCl is a main component of the total inorganic chlorine (Cl_y), defined as $Cl_y \simeq$ HCl + ClO + chlorine nitrate ($ClONO_2$), inside the Antarctic vortex in spring, owing to low ozone values. To confirm the quality of two SMILES level 2 (L2) data products provided by the Japan Aerospace Exploration Agency (JAXA) and Japan's National Institute of Information and Communications Technology (NICT), vis-à-vis the partitioning of Cl_y, comparisons are made using other satellite data from the Aura Microwave Limb Sounder (MLS) and Atmospheric Chemistry Experiment Fourier Transform Spectrometer (ACE-FTS). HCl values from the SMILES NICT L2 product agree to within 10 % (0.3 ppbv) with the MLS HCl data between 450 and 575 K levels in PT and with the ACE-FTS HCl data between 425 and 575 K. The SMILES JAXA L2 product is 10 to 20 % (0.2–0.5 ppbv) lower than that from MLS between 400 and 700 K and from ACE-FTS between 500 and 700 K. For ClO in daytime, the difference between SMILES (JAXA and NICT) and MLS is less than ±0.05 ppbv (100 %) between 500 K and 650 K with the ClO values less than 0.2 ppbv. $ClONO_2$ values as measured by ACE-FTS also reveal 0.2 ppbv at 475–500 K level, resulting in the HCl / Cl_y ratios of 0.91–0.95. The HCl / Cl_y ratios derived from each retrieval agree to within −5 to 8 % with regard to their averages. The high HCl values and HCl / Cl_y ratios observed by the three instruments in the lower stratospheric Antarctic vortex are consistent with previous observations in late Austral spring.

Published by Copernicus Publications on behalf of the European Geosciences Union.

1 Introduction

Hydrogen chloride (HCl) and chlorine monoxide (ClO) play an important role in the mechanism of ozone destruction in the stratosphere. The total inorganic chlorine (Cl_y) in the stratosphere is defined as the sum of the volume mixing ratios of Cl, $2\times Cl_2$, ClO, HOCl, $2\times$ClOOCl, OClO, chlorine nitrate ($ClONO_2$), and HCl. Observing the time evolution of these species in both the Arctic and Antarctic vortices (lower stratosphere) is essential since HCl and $ClONO_2$ act as reservoirs for the chlorine radicals (ClOx = Cl + ClO + $2\times$ClOOCl) that destroy ozone catalytically (e.g., WMO, 2007). It is also useful to evaluate model studies of the time series of Cl_y species (e.g., Santee et al., 2008b). The reservoirs, HCl and $ClONO_2$, are decomposed to yield Cl_2 through heterogeneous reactions occurring in/on sulfate aerosols and polar stratospheric clouds (PSCs) in winter. Consequently, ClOx is elevated through photolysis/photochemical reactions in winter/spring, then it is deactivated into the reservoirs.

Increased amounts of HCl in the springtime Antarctic when ClOx is deactivated were observed by ground-based Fourier Transform Infrared Spectroscopy (FTIR) instruments starting in 1987 (e.g., Murcray et al., 1989; Liu et al., 1992; Kreher et al., 1996). Using satellite instruments on board the Upper Atmosphere Research Satellite (UARS) in the 1990s, several studies showed the time evolution of ClO and HCl in the spring Antarctic vortices (e.g., Douglass et al., 1995; Santee et al., 1996; Chipperfield et al., 1996; Grooß et al., 1997; Mickley et al., 1997). On 3–12 November 1994, measurements from the Atmospheric Trace MOlecule Spectroscopy (ATMOS) on the Space Shuttle were conducted. Rinsland et al. (1996) and Michelsen et al. (1999) suggested that the high HCl/Cl_y ratio (~ 0.9) was maintained in the Antarctic vortex. Also, in November 1996, it was reported that the high HCl and low $ClONO_2$ were observed by HALogen Occultation Experiment (HALOE) and Improved Limb Atmospheric Spectrometer (ILAS) satellite instruments, respectively (Hayashida and Sugita, 2007). All of these results confirm a theoretical study by Prather and Jaffe (1990) who showed a mechanism for increased HCl values after the "ozone hole" period in the Antarctic. This can be understood as low values of ozone shifting the partitioning of ClOx into Cl, so that the reaction Cl + CH_4 that forms HCl proceeds faster than the reaction ClO + NO_2 + M that forms $ClONO_2$, thus reaching a steady state with a high HCl/Cl_y ratio (see Sect. 4.3). In addition, there was indirect evidence of increased values of HCl in the Antarctic in October 1993 from aircraft measurements of the isotopic composition of CO (Müller et al., 1996; Brenninkmeijer et al., 1996).

Simultaneous in situ aircraft measurements of ClO, HCl, and $ClONO_2$ have been available since 1997 (Bonne et al., 2000). An aircraft mission was performed in the 1999/2000 Arctic winter; the time evolution of the Cl_y species has been investigated (e.g., Wilmouth et al., 2006). Dufour et al. (2006) also showed an evolution of the Cl_y partitioning in the 2004/2005 Arctic winter from the Atmospheric Chemistry Experiment-Fourier Transform Spectrometer (ACE-FTS) measurements. However, the HCl value or HCl/Cl_y ratio in the Arctic was lower than those in the Antarctic (e.g., Santee et al., 2008b; Manney et al., 2011; Wegner et al., 2012), even with severe ozone loss in the 2010/2011 Arctic winter (e.g., Manney et al., 2011). An exception was the 1996/1997 Arctic winter when the breakup of the vortex occurred in May; an HCl/Cl_y ratio of 0.8–0.9 was observed by HALOE (Douglass and Kawa, 1999; Konopka et al., 2003). Very low ozone values in the Antarctic play a central role in the difference in Cl_y partitioning between the Arctic and the Antarctic (e.g., Douglass et al., 1995), except in the unusual Antarctic winter 2002, when some deactivation into $ClONO_2$ occurred (e.g., Grooß et al., 2005; Höpfner et al., 2004).

In the Antarctic, no comprehensive aircraft campaign has been done since the 1994 mission (Tuck et al., 1997; Jaeglé et al., 1997), so satellite measurements are crucial to study the partitioning of Cl_y in the Antarctic. Although a high HCl/Cl_y ratio is usually seen in the upper stratosphere, it has also been seen in the lower stratosphere in the combined data from the Aura Microwave Limb Sounder (MLS) and ACE-FTS data (WMO, 2007; Santee et al., 2008b) or just in the MLS data (Santee et al., 2011; de Laat and van Weele, 2011) since 2004. This is due to the combination of diabatic descent of air inside the vortex, low ozone values, and isolation of the lower stratospheric vortex.

The International Space Station (ISS) borne instrument, the Superconducting Submillimeter-Wave Limb-Emission Sounder (SMILES), started operations in October 2009. SMILES observed latitudes between $\sim 66^\circ$ N and $\sim 38^\circ$ S. On 19–24 November 2009, there were, however, measurements including the Antarctic ($\sim 38^\circ$ N to $\sim 66^\circ$ S) due to the ISS observation geometry (see Sect. 2.1). The breakup of the Antarctic vortex in the lower stratosphere occurred in December 2009 (NOAA, 2009), so that some measurements were taken inside the vortex where high HCl values are expected. In this paper, we focus on these SMILES measurements, and analyze the vertical profiles of HCl and ClO inside the Antarctic vortex to confirm those data quality vis-à-vis the partitioning of Cl_y, through comparisons with satellite data for the same time period from the MLS and ACE-FTS instruments. Comparisons performed when the HCl value is high (~ 3 ppbv) in the lower stratosphere will provide valuable information on the HCl measurements.

Data from satellite measurements used here are described in Sect. 2. The methodology of the study is mentioned in Sect. 3. Vertical profiles of HCl, ClO, and HCl/Cl_y ratio are shown in Sect. 4 and discussion of the Cl_y partitioning, including the diurnal changes in ClO and $ClONO_2$, is also given in Sect. 4. The conclusions of the study are summarized in Sect. 5.

2 Satellite measurements

2.1 SMILES

SMILES is a passive sensor to measure the limb of Earth's atmosphere in the frequency bands around 625 GHz and 650 GHz. The instrument was attached to the Japanese Experiment Module (JEM) on board ISS. The emission lines of O_3, HCl, ClO, HO_2, HOCl, BrO, and other molecules can be found in the low-noise spectra obtained with a 4 K mechanical cooler and superconductor-insulator-superconductor (SIS) mixers. The SMILES observations started on 12 October 2009 and ceased on 21 April 2010 due to the failure of a critical component in the submillimeter local oscillator. Results from SMILES have demonstrated its high potential for observing atmospheric minor constituents in the middle atmosphere, as shown in Kikuchi et al. (2010).

Because the ISS is in a non-sun-synchronous circular orbit with an inclination angle of 51.6° to the Equator, the SMILES measurements at each tangent point occur at various local solar times (LST). For several specific periods, including 19–24 November 2009, the ISS rotated 180° around its yaw axis, and thus the observation latitude range was shifted to southern high latitudes up to 66° S. A more detailed description of the observation latitudes and periods is found in Fig. 1 of Kasai et al. (2013). There were also southern high latitude measurements on 10–19 February and 8–17 April 2010.

Since SMILES has three specified detection bands – 624.32–625.52 GHz (Band A), 625.12–626.32 GHz (Band B), and 649.12–650.32 GHz (Band C) – with two acousto-optical spectrometers, observations of Bands A, B, and C are made on a time-sharing basis, such as Bands A+B, A+C, or B+C. In the period that we analyze, Bands B+C measurements were performed. The $H^{35}Cl$ rotational transition ($J = 1$–0) is located at 625.9 GHz in Band B. The ClO transitions in the ground ro-vibronic state ($J = 35/2$–$33/2$) are located at 649.445 GHz and 649.451 GHz in Band C. Vertical resolution is 3.5–4.1 km and vertical range of the measurements is from $\sim$ 12 km to 96 km.

The SMILES level 2 (L2) data processing systems (Takahashi et al., 2010; Baron et al., 2011) retrieve vertical profiles of the atmospheric minor constituents from the calibrated radiance observations (Level 1b data, hereafter referred to as L1b). In this paper, we used two SMILES L2 data products, which are separately processed with different retrieval algorithms: the version 2.1 (hereafter referred to as v2.1) of JAXA L2 products (Mitsuda et al., 2011) (hereafter SMILES-JAXA) and the v2.1.5 of NICT L2 products (Kasai et al., 2013; Sagawa et al., 2013) (hereafter SMILES-NICT). Both of the data sets were publicly released on 5 March 2012 (http://smiles.tksc.jaxa.jp/ for SMILES-JAXA and http://smiles.nict.go.jp/ for SMILES-NICT).

Both of the retrieval algorithms used same L1b data and similar instrument functions in the forward model calculations. The vertical inversion of the volume mixing ratio profiles are based on the optimal estimation method (e.g., Rodgers, 2000). However, several differences in the two algorithms made different data products (Kasai et al., 2013; Sagawa et al., 2013). Thus, it is of importance to compare both of the L2 products to investigate matters relating to the algorithms. Here, we briefly present the differences that affect mostly the lower stratosphere data quality.

One of the major differences is the spectral bandwidth used in the retrieval analysis. The SMILES-JAXA L2 algorithm uses a full bandwidth ($\sim$ 1.2 GHz) of each detection band to simultaneously retrieve all the observed species in that band. On the other hand, SMILES-NICT processing employs the sequential retrieval approach using a narrow bandwidth around the targeted species (Baron et al., 2011). For example, after O_3 and temperature profiles were retrieved, HCl is retrieved from the spectra extracted at $\pm$300 MHz of the HCl line center. ClO is retrieved from the spectra in Band C using a spectral bandwidth of 400 MHz centered on the ClO line. For the species of interest in this paper (HCl and ClO), the information in the lower stratosphere can be retrieved also from the far wings of their lines. Therefore, the usage of a limited spectral bandwidth results in a decrease of the sensitivity and degradation of the vertical resolution at lower altitudes (Sagawa et al., 2013). Whereas, for the full bandwidth approach, it is difficult to deal with nonlinearity of the detector in the far wings. Both of the approaches, thus, have some disadvantages.

Different assumptions on a priori state also introduce systematic biases on retrieved profiles, particularly when the measurement sensitivity is low. The a priori profile of SMILES-JAXA is based on mean profiles for month, latitude, (daytime and nighttime separately for ClO), using the MLS version 2.2 data. The MLS ClO data have been bias-corrected as suggested by Santee et al. (2008a). SMILES-NICT used a single common a priori profile for HCl or ClO for all observations. However, as stated in Sect. 4.1, the impact of the difference on the retrieved HCl values is insignificant because of the high sensitivity of the measurements studied here.

For the modeling of continuum absorptions of H_2O and dry air, SMILES-JAXA uses the MPM-93 model (Liebe et al., 1993) with a scaling factor of 1.34. SMILES-NICT uses a model on the basis of Pardo et al. (2001). The dry air continuum absorption coefficient was increased by a factor of 20 % from the original formula, and retrieves H_2O as the continuum (Kasai et al., 2013). The above differences employed in each retrieval processing could be the cause of differences in the results of retrieved volume mixing ratio profiles. There are other lower stratospheric differences in the SMILES-JAXA and SMILES-NICT processing: the approach for measurement tangent height correction, a priori state of temperature and pressure, and so on. More detailed descriptions of these differences are found elsewhere (Kasai et al., 2013; Sagawa et al., 2013). There are also differences

in spectroscopic parameters used in each forward model; however, the impact of the differences on the retrieved data products seems to be small in the lower stratosphere, as shown in Sagawa et al. (2013) for ClO and Yokoyama et al. (2013) for HCl. A list of the parameters, namely the line frequency ν_0, the air broadening coefficient $\gamma_{\rm air}$, and its temperature dependence $n_{\rm air}$, is shown in Table 1.

We present error analysis and validation results for both HCl and ClO achieved thus far. For previous versions of SMILES-JAXA, precision is 10 % at 15 km and 1 % at 30 km for HCl (Kikuchi et al., 2010; Shiotani et al., 2010). For ClO, precision is estimated to be 10 pptv between 19 and 28 km (Suzuki et al., 2012). This is evaluated from the standard deviation of the nighttime ClO measurements. The mean nighttime data also provide a good measure for a bias estimation of the JAXA ClO data products, which has already shown a validity for the BrO data product (Stachnik et al., 2013). This bias will be considered for ClO later (Sect. 4.2). The cause of this bias is unknown, but it seems to be due to an unexpected quadratic spectral baseline of the L1b data, which should be flattened by calibration, and a small residual between L1b and the forward model calculation, which could also arise from the quadratic continuum emission feature (Suzuki et al., 2012). The full-bandwidth approach used in the JAXA processing system tends to be susceptible to these baseline-related effects. Validation studies for SMILES-JAXA are, to date, in preparation.

For HCl from SMILES-NICT (v2.1.5), the precision is estimated to be $\sim$1–2 % at the 10 hPa level and it increases to 8 % at 80 hPa. The validation of SMILES-NICT HCl was performed by comparing with MLS version 3.3 data and ACE-FTS version 3.0 data (Yokoyama et al., 2013): the absolute difference between SMILES-NICT and MLS amounts to –0.2 ppbv at 80 hPa and +0.1 ppbv at 10 hPa. The absolute difference between SMILES-NICT and ACE-FTS ranges from zero to +0.1 ppbv at 80–10 hPa levels. For ClO from SMILES-NICT (v2.1.5), the precision is estimated to be 100 pptv and 30 pptv between 100 hPa and 10 hPa (Sato et al., 2012). Sagawa et al. (2013) have also estimated the bias uncertainty of 5–10 pptv below 20 hPa level and made a validation study: the absolute differences between SMILES-NICT and MLS version 3.3 data or Odin Sub-Millimeter Radiometer (SMR) Chalmers Version 2.1 data (Murtagh et al., 2002) is within $\pm$0.1 ppbv at 80–10 hPa levels.

We analyzed SMILES data obtained on 19–24 November, when the measurements were conducted between 38° N and 66° S. During those days, the polar vortex was somewhat shifted toward South America, so that the edge of the vortex reached to around 50° S in the lower stratosphere (de Laat et al., 2010). Therefore, we extracted the SMILES data between 50° S and 66° S. The profiles of SMILES (both JAXA and NICT) were discarded when flagged with "field-of-view interference" and "altitude error" according to a release note (http://smiles.tksc.jaxa.jp/l2data/index_e.html). For SMILES-JAXA, profiles with "convergence" value greater than 10 are discarded. Further, data points with precision larger than a half of a priori error are also discarded. For SMILES-NICT, profiles with "chi-square" value larger than 0.8 are discarded. For the NICT retrieval, chi-square is the summation of the squared and variance weighted residuals in the measurement space and the null space after they are normalized by the number of measurements and retrieval parameters. Typical chi-square values are smaller than unity because of the overestimation of the measurement noise (Baron et al., 2011). Thus, no good retrievals have been discarded by this data selection. Data points with measurement response smaller than 0.8 are also discarded.

Table 1. Spectroscopic parameters for HCl and ClO in the SMILES forward models (see Sect. 2.1).

	ν_0 (MHz)	$\gamma_{\rm air}$ (MHz/hPa)	$n_{\rm air}$
	$H^{35}Cl$		
JAXA	625901.6584[a]	2.54[b]	0.72[b]
	625918.6975[a]		
	625932.0081[a]		
NICT	625901.6627[c]	2.54[d]	0.72[d]
	625918.7020[c]		
	625931.9977[c]		
	ClO		
JAXA	649445.250[e]	2.11[e]	0.85[e]
	649451.072[e]		
NICT	649445.040[d]	2.15[d]	0.77[d]
	649451.170[d]		

[a] Perrin et al. (2005), [b] Read et al. (2004), [c] Cazzoli and Puzzarini (2004), [d] an original laboratory study; see Baron et al. (2011), [e] Oh and Cohen (1994).

2.2 MLS

Since August 2004, the MLS instrument on the National Aeronautics and Space Administration (NASA) Earth Observing System (EOS) Aura satellite (Waters et al., 2006) has operated between 82° N and 82° S. MLS measures millimeter- and submillimeter-wavelength thermal emission from the limb of Earth's atmosphere. We used HCl and ClO data products retrieved with the version 3.3 data processing algorithm (Livesey et al., 2006), which are publicly available from http://mls.jpl.nasa.gov/. The quality of the HCl data is as follows (Livesey et al., 2011): vertical resolution in the lower stratosphere is $\sim$3 km and precision is 0.3–0.2 ppbv at 100–10 hPa. The quality of the ClO data is as follows (Livesey et al., 2011): vertical resolution is 3.0–4.5 km, precision is $\pm$0.3 ppbv at 147 hPa and $\pm$0.1 ppbv at 100–22 hPa, and bias estimates are from $-$0.1 to zero ppbv at 50–70° S in November. In this study, we used data taken at 50–66° S on

19–24 November 2009. Data screening is also done according to Livesey et al. (2011).

2.3 ACE-FTS

ACE-FTS, the primary instrument on the SCISAT-1 satellite, is a high-resolution infrared Fourier transform spectrometer that measures solar occultation spectra between 2.2 and 13.3 µm (Bernath et al., 2005). The observations began in February 2004. It has also operated in the period of 19–24 November at latitudes between 65.7° S and 69.3° S. This is a somewhat more southerly latitude than SMILES and MLS measurements used in this study. Vertical resolution is 3–4 km. We used HCl and $ClONO_2$ data products retrieved with the version 3.0 data processing algorithm (Boone et al., 2005) (http://www.ace.uwaterloo.ca/). The error analysis of the HCl data has not yet been evaluated, but the measurement variability that provides an upper limit on retrieval precision is estimated to be on the order of 5 % at 20–55 km (Mahieu et al., 2008). The fitting error of the $ClONO_2$ data is below 10 % at 20–30 km and increases to 40 % at 14 km (Wolff et al., 2008). Dufour et al. (2006) have provided an error budget for a single occultation: the total errors for HCl and $ClONO_2$ are, respectively, estimated to be 4–7 % and 10–19 % between 16.5 km and 28.5 km.

2.4 MIPAS

The Michelson Interferometer for Passive Atmospheric Sounding (MIPAS) on board ESA's Envisat is a mid-infrared emission spectrometer (Fischer et al., 2008). The observations were performed from July 2002 to April 2012. We used the Institute for Meteorology and Climate Research (IMK)/Instituto de Astrofísica de Andalucía (IAA) $ClONO_2$ data product, version V5R_CLONO2_220 (von Clarmann et al., 2009, 2013). The vertical resolution at the tangent altitude of 20 km is ∼ 3 km, and the precision between 15 and 25 km is ∼ 8 % (von Clarmann et al., 2009). This data set is used for an interpretation of the diurnal cycle of Cl_y species, as described in Sect. 4.3.

3 Method

In order to show the quality of the SMILES data for studying Cl_y partitioning inside the Antarctic vortex, we have made comparisons with the other satellite data sets described above. The 2009 Antarctic vortex at 450 K potential temperature (PT) level exhibited a typical seasonal pattern: it developed in mid-May, maximized around September, and then diminished in the late November/December period (NOAA, 2009).

To extract observed data only inside the Antarctic vortex, we used derived meteorological products (DMPs) (Manney et al., 2007). For both the MLS and ACE-FTS measurement locations and times, DMPs are produced to facilitate comparisons between different satellite instruments. They include PT, potential vorticity (PV), equivalent latitude (EqL), horizontal winds, and tropopause locations. The EqL is the latitude that would enclose the same area between it and the pole as a given PV contour (Butchart and Remsberg, 1986). In this study, we used DMPs derived from the NASA Global Modeling and Assimilation Office (GMAO) Goddard Earth Observing System (GEOS) data set (version 5), hereafter referred to as GEOS-5 (Reinecker et al., 2008). Using DMPs to view measurements with respect to their air mass characteristics is valuable in a study of chemistry and dynamics inside/outside the vortex. To compare SMILES measurements with those from MLS and ACE-FTS, we also obtained DMPs for the SMILES measurements for the study period.

We used PT for a vertical coordinate, since we focus on the observations in the lower stratosphere, where Cl_y has a much longer chemical lifetime compared to the transport timescale at this time and location. In this study, we constructed averaged "vortex profiles" using data points at each vertical level that are poleward of the vortex edge center shown in the each DMP file. For instance, the vortex edge center is located at $\sim -65°$ EqL (negative values are assigned in the Southern Hemisphere) at the 490 K PT level. The resulting EqL values around 490 K inside the Antarctic vortex are, on average, $-71°$ EqL, $-76°$ EqL, and $-75°$ EqL for SMILES, MLS, and ACE-FTS observations, respectively. The volume mixing ratio of tracer species mapped with respect to the PT and EqL is nearly constant with EqL over a certain PT range within the vortex (e.g., Fig. 5 of Lingenfelser and Grose, 2002).

For the SMILES and ACE-FTS data, PT values from the DMPs are assigned at each altitude grid point, whereas for the MLS data, PT values from the DMPs are assigned at each pressure grid point. The averaged profiles are calculated from data contained within a 25 K wide PT bin. In general, intercomparison among satellite measurements is a difficult task because of the different vertical and horizontal resolutions considered (e.g., Ceccherini et al., 2003; Ridolfi et al., 2006). Thus, any interpolation of data onto specific PT levels has not applied in this study. In addition, the uncertainty in the meteorological data should also be concerned in such a comparison study. However, it was suggested that the GEOS-5 temperatures have about 1 K low bias (Lambert et al., 2012), which has a small impact on the calculation of PT. The pointing uncertainty in the tangent altitude was estimated to be 340 m, 150 m, and 150 m for SMILES, MLS, and ACE-FTS, respectively (Kikuchi et al., 2010; Cofield and Stek, 2006; Harrison and Bernath, 2013). These uncertainties are inherent in the constructed average profiles. The individual profiles from SMILES HCl / ClO, MLS HCl / ClO, and ACE-FTS HCl / $ClONO_2$ used for the averages are found in Sugita et al. (2012).

Figure 1 shows measurement latitudes as a function of LST used in this study (data taken inside the vortex). As mentioned in Sect. 2.1, the SMILES measurements occur at

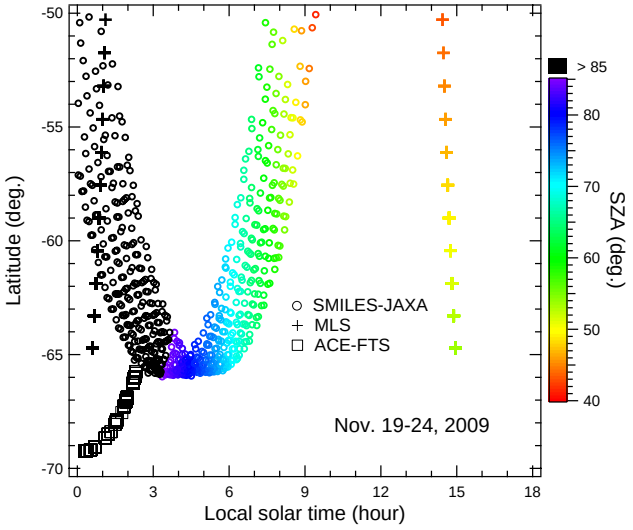

Fig. 1. Measurement latitude as a function of local solar time for SMILES (open circles), MLS (crosses), and ACE-FTS (open squares). Solar zenith angle (SZA) is color-coded between 40° and 85°. Above 85°, the symbols are coded in black. Data only inside the Antarctic vortex (within the edge center) between 19 and 24 November 2009 are used.

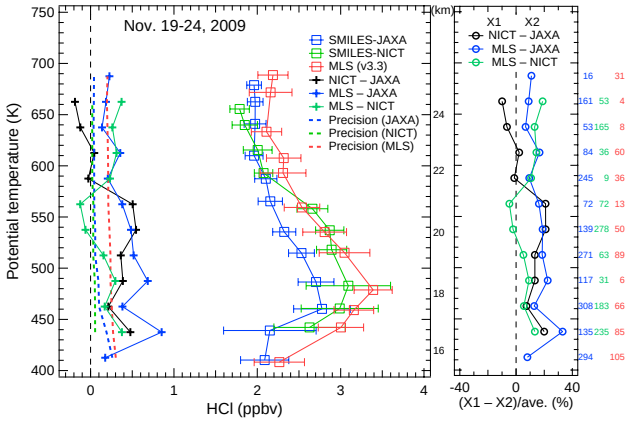

Fig. 2. Vertical profiles, as a function of potential temperature (PT), of HCl volume mixing ratios as measured by SMILES and MLS on 19–24 November 2009 inside the vortex (within the edge center). The left panel shows average profiles of HCl in each 25 K PT bin (each vertical bar corresponds to 25 K) for the SMILES-JAXA (blue), SMILES-NICT (green), and MLS (red) data products. Squares and horizontal bars show average and $\pm 1\sigma$ standard deviations, respectively. Dashed lines show reported precisions. The black crosses show the absolute difference between the two SMILES products. The blue and green crosses show the absolute difference between the MLS and SMILES-JAXA or SMILES-NICT, respectively. Approximate altitudes corresponding to PT are shown on the right-hand side of the panel. The right panel shows the relative difference with regard to the absolute difference divided by its mean value of SMILES-JAXA and SMILES-NICT, MLS and SMILES-JAXA, or MLS and SMILES-NICT products. The numbers of data used in the averages are also listed outside of the right panel: SMILES-JAXA (blue), SMILES-NICT (green), and MLS (red).

various LST. Therefore, it is crucial to consider the diurnal cycle of ClO and $ClONO_2$ in comparisons between SMILES, MLS, and ACE-FTS. In the following section, we consider SMILES and MLS ClO data only for solar zenith angles (SZAs) less than 85°, representing daytime measurements. The daytime measurements from SMILES occurred at LSTs between 03:00 and 09:00 LST, whereas the daytime measurements from MLS occurred at LSTs of 14:00–15:00 LST. These LST differences are carefully treated in the following discussion. Data with SZAs larger than 85° are coded in black for each symbol. For ACE-FTS measurements, all of the occultations occurred at a SZA of 90° from the satellite sunset for this time and location.

4 Results and discussion

4.1 HCl

Figure 2 shows the vortex profiles of SMILES and MLS HCl volume mixing ratios taken on 19–24 November 2009 at latitudes between 50° S and 66° S as a function of PT. PTs of 400, 500, 600, and 700 K approximately correspond to altitudes of 15, 19, 23, and 26 km, respectively. Data are averaged within the PT bin between 400–425 K and 675–700 K. At first, we focus on the results from SMILES. The average and one sigma standard deviation are shown for both SMILES-JAXA and SMILES-NICT data in the left panel (blue and green squares, respectively). The absolute differences between the SMILES-JAXA and SMILES-NICT averages in each bin are also shown in the same panel (black crosses). Precision was calculated as an average derived from the measurement precision reported for the respective data files, and is shown as the dashed line: it is quite small compared to the retrieved value. The right panel shows the relative difference expressed as the absolute difference divided by the mean of SMILES-JAXA and SMILES-NICT data (black circles). The data values used in each bin are shown on the right-hand side of the right panel. Since the PT interval is narrower than the retrieval grids, these numbers are nonuniform in the vertical range.

The peak value of SMILES HCl reveals 2.8 and 3.1 ppbv at 450–475 K bin (JAXA) and 475–500 K bin (NICT), respectively. The relative difference between SMILES-JAXA and SMILES-NICT amounts to 7–21 % between 425–450 K and 550–575 K bins (the absolute difference up to 0.5 ppbv), and −10 to 2 % between 575–600 K and 650–675 K bins, resulting in a better agreement than in the lower PT levels. The cause of these differences of up to 20 % found in the lower levels is unclear, but it is related to the different approaches used in the forward models and retrieval schemes described in Sect. 2.1. Besides the difference in the spectral bandwidth

used in the retrieval analysis, another possible cause could be the different a priori profiles used for each algorithm. We have tested JAXA's processing system using a more realistic a priori (constructed from the MLS version 2.2 HCl data inside the Antarctic vortex). However, the result was almost the same because the measurement sensitivity is sufficiently high that the retrieval is insensitive to the a priori. Another contributing factor may be the difference in dealing with the modeling of continuum absorptions (see Sect. 2.1). A further investigation to quantify the difference is ongoing along with updates of both retrieval algorithms.

To compare these SMILES HCl data products with those from other satellite instruments, the Aura MLS and ACE-FTS HCl data are analyzed. Figure 2 also shows the vortex profiles of MLS HCl (red squares). The maximum mixing ratio of MLS is seen at 475–500 K bin with a value of 3.4 ppbv. The shape of the profile is similar to that of SMILES-NICT. Better agreement is found between SMILES-NICT and MLS (green crosses) than from SMILES-JAXA and MLS (blue crosses). The relative difference between SMILES-NICT and MLS ranges from −5 to 13 % between 425–450 K and 575–600 K bins, but it increases to 19 % at 650–675 K bin. For SMILES-JAXA and MLS, the relative difference amounts to 7–23 % between 400–425 K and 675–700 K bins, except for 33 % at 425–450 K bin. In the period of November 2009, band 13 (primary to detect $H^{35}Cl$) of the MLS instrument was not used and HCl was retrieved using band 14; it has been suggested that retrievals of HCl from band 14 have a high bias at high HCl values (above ∼ 3 ppbv) (Livesey et al., 2011). The positive difference found in both of the comparisons between SMILES and MLS at 450–500 K might reflect an artifact of the MLS band 14 measurement to some extent.

Figure 3 shows the vortex profiles of SMILES and ACE-FTS HCl taken on 19–24 November 2009 as a function of PT. The SMILES data are identical to those shown in Fig. 2. Since the ACE-FTS measurements are made using solar occultation, observations are limited to a certain latitude in a certain period (see Sect. 3 and Fig. 1). The number of observations (occultation events) inside the vortex for ACE-FTS is 26. Since we used the 1 km altitude grid data, some profiles have two data points in a bin. Thus, the number of data used in the 400–425 K bin is 29 at the maximum. The maximum mixing ratio of ACE-FTS is seen at 500–525 K bin with a value of 2.9 ppbv that is similar to the results from SMILES and MLS, with a slightly higher PT level than those of SMILES and MLS.

The relative difference between SMILES-JAXA and ACE-FTS (blue circles) ranges from −5 % to 19 %. The relative difference between SMILES-NICT and ACE-FTS (green circles) ranges from −9 % to −1 % between 425–450 K and 500–575 K bins, but it increases to 16–22 % between 575–600 K and 650–675 K bins. In summary, a general feature is that SMILES-JAXA HCl is somewhat lower than both MLS and ACE-FTS, whereas SMILES-NICT HCl shows better agreement with both MLS and ACE-FTS between 425 K and

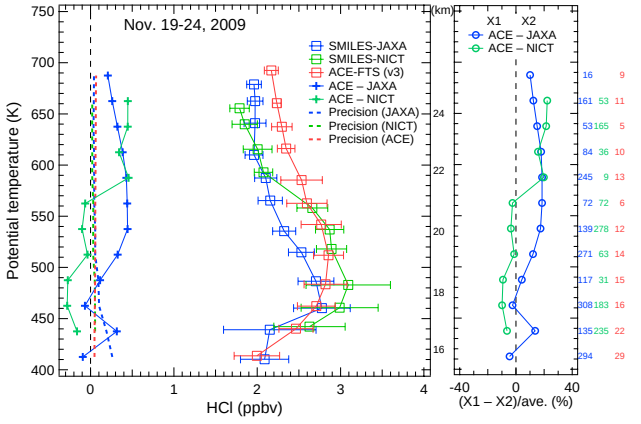

Fig. 3. Same as Fig. 2, but for SMILES and ACE-FTS. The absolute and relative differences between SMILES-JAXA and SMILES-NICT are omitted.

575 K. Above 575 K, SMILES-NICT HCl is, however, lower than that from both MLS and ACE-FTS.

The HCl values from MLS and ACE-FTS agree to within 10 % above 550 K (not shown). In general, both SMILES retrievals are a maximum of 23 % smaller than MLS and ACE-FTS at these levels.

4.2 ClO

Figure 4 shows the vortex profiles of the daytime ClO volume mixing ratios as measured by SMILES and MLS on 19–24 November 2009 at latitudes between 50° S and 66° S as a function of PT. Generally, both the SMILES-JAXA and SMILES-NICT profiles show increasing values up to 0.1–0.2 ppbv at 625–700 K with increasing altitudes. Below 600 K level, the ClO values were less than 0.1 ppbv. For the SMILES-JAXA ClO product, the bias should be corrected, as mentioned in Sect. 2.1. For this latitude and period considered here, the bias is estimated to be −33 pptv at 16 km and negligibly small above 19 km. Thus, this value (33 pptv) is added before taking the average at 16 km (400–450 K level). The absolute difference between SMILES-JAXA and SMILES-NICT ClO is ±0.05 ppbv between 450–475 K and 600–625 K bins, although the difference between the two products amounts to −0.07 ppbv at 625–675 K and 0.07 ppbv at 425 K. The ClO values themselves are as small as 0.1–0.2 ppbv, making large relative differences.

In Fig. 4, the MLS ClO is also averaged only from measurements taken with SZAs less than 85° (see Fig. 1). Similar to the results from SMILES, the daytime MLS ClO values increased to ∼ 0.35 ppbv at 675–700 K bin. The reported precisions and one sigma standard deviations of the data are smaller in SMILES than in MLS, reflecting the difference in system noise temperatures between the two instruments (Kikuchi et al., 2010). It should be noted that some negative values in the MLS data are found below the 500 K level.

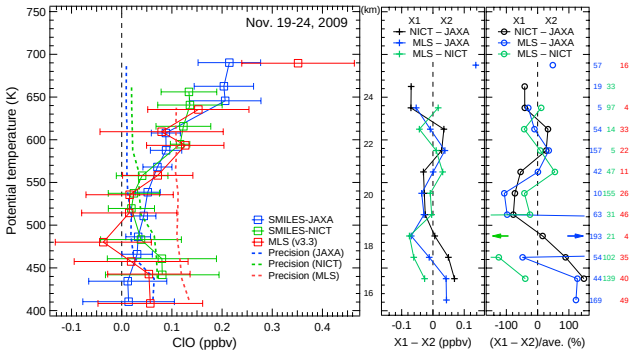

Fig. 4. Same as Fig. 2, but for ClO volume mixing ratios as measured by SMILES and MLS. For clarity, absolute differences are shown in the middle panel. Measurements with solar zenith angles less than 85° (daytime) are used. Arrows in the right panel show larger relative differences owing to the averages close to zero.

We have bias-corrected with 0.09–0.15 ppbv (added) below 500 K (100 hPa and 68 hPa levels), depending on latitudes (5-degrees bin) for each ClO data before taking the averages, as suggested by Livesey et al. (2011). The absolute difference between SMILES and MLS ClO is almost ±0.05 ppbv between 400 K and 650 K, although the values themselves are again below 0.15 ppbv, making large relative differences. Although the number of data points is small, the SMILES ClO values in the SZA range between 85° and 95° are zero to 0.05 ppbv between 400 K and 700 K levels. For measurements with SZAs larger than 95°, ClO reveal values around zero.

As shown in Fig. 1, the MLS observations were taken at 14:00–15:00 LST, whereas the SMILES observations were taken at 03:00–09:00 LST. Thus, a large difference (0.14 ppbv) between SMILES-JAXA and MLS at 675–700 K bin (∼ 26 km) could be partly associated with diurnal changes in ClO. At this altitude, time, and location, the diurnal cycle of ClO is thought to take place via the photolysis of $ClONO_2$ (Santee et al., 2008b). Indeed, if we take an average only using the SMILES-JAXA ClO data with SZAs less than 55° in the 675–700 K bin (the number of data is 5 out of 57), the ClO value of 0.21 ppbv (SZAs less than 85°) varies to 0.30 ppbv. As a result, the absolute difference between SMILES-JAXA and MLS in the 675–700 K bin becomes from 0.14 ppbv to 0.05 ppbv, revealing better agreement (not shown). Therefore, the SZA or LST difference found in comparison to ClO within the daytime should be carefully treated at this altitude. A further discussion of the diurnal changes in ClO and $ClONO_2$ is provided in the next subsection.

4.3 Cl_y partitioning

Since Cl_y in the stratosphere in 2009 was ∼ 3.3–3.5 ppbv (WMO, 2011), it is clear that HCl dominates Cl_y in this altitude range and time period. Such a feature is usually not seen in the lower stratosphere, but is seen in the upper stratosphere ($Cl_y \simeq$ HCl) (e.g., WMO, 2011). This high HCl occurs as a result of low O_3 values ("ozone hole") in October, as follows (e.g., Mickley et al., 1997). The two competing reactions of the NO radical,

$$NO + ClO \rightarrow Cl + NO_2 \quad (R1)$$

$$NO + O_3 \rightarrow O_2 + NO_2, \quad (R2)$$

are the key to understanding this behavior. Under "ozone hole" conditions with low O_3 and high ClO values, Reaction (R1) becomes faster than Reaction (R2), allowing increased values of Cl. The low O_3 values directly slow the reaction:

$$Cl + O_3 \rightarrow ClO + O_2\,. \quad (R3)$$

Thus, the production of HCl occurs from September to October through the following reaction:

$$Cl + CH_4 \rightarrow HCl + CH_3 \quad (R4)$$

as shown in, e.g., Santee et al. (2008b). HCl production is thus sensitive to the amount of O_3. A recent theoretical study suggests that this conversion is quite rapid in the Antarctic vortex through Reaction (R4) and a reaction Cl + CH_2O (Grooß et al., 2011).

HCl is destroyed through reactions with the OH radical and on the surface of sulfate aerosols, but both are so slow that the chemical lifetime of HCl is long compared to the transport time in November (i.e., high HCl values should be found as long as the vortex exists).

Figure 5 (left panel) shows vertical profiles of ClO, $ClONO_2$, and HCl inside the vortex on 19–24 November 2009, summarizing Figs. 2, 3, and 4. The bars show the one sigma standard deviation of data for each average. For the ACE-FTS $ClONO_2$ data, the same occultation measurements are used in the average as were used for the HCl data. It is of importance to examine Cl_y species other than HCl and ClO. Because of Reactions (R1) through (R4), the formation of $ClONO_2$ by ClO + NO_2 + M should also be suppressed significantly inside the vortex where the HCl value is high at 450–500 K level (e.g., Prather and Jaffe, 1990). Indeed, the ACE-FTS $ClONO_2$ values are less than 0.3 ppbv below 475–500 K bin, as shown in Fig. 5. Above the 500–525 K level, $ClONO_2$ increases with altitude to 1.1–1.2 ppbv at 650–700 K.

The ratio of HCl to Cl_y is shown in the right panel of Fig. 5. We take composite Cl_y values as computed by the equations below:

$$Cl_y(\mathrm{SMILES}) = \mathrm{HCl(SMILES)} + \mathrm{ClO(SMILES)} \quad (1)$$

$$+ ClONO_2(\mathrm{ACE-FTS})$$

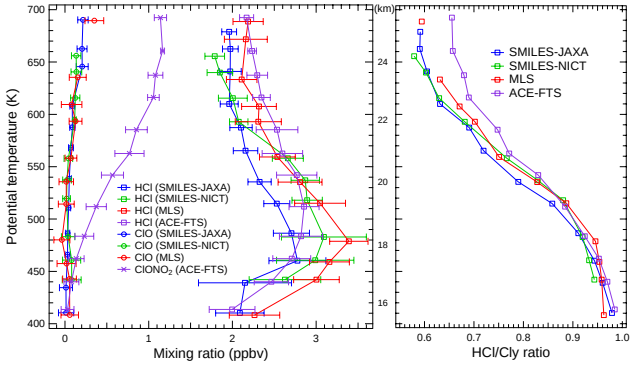

Fig. 5. Vertical profiles of ClO (measured by SMILES and MLS), $ClONO_2$ (measured by ACE-FTS), and HCl (measured by SMILES, MLS, and ACE-FTS) on 19–24 November 2009 inside the Antarctic vortex (within the edge center) as a function of potential temperature, PT (left panel). Horizontal bars show $\pm 1\sigma$ standard deviations of the averages. Approximate altitudes corresponding to PT are shown on the right-hand side of the panel. HCl/Cl_y ratios computed for each of the three instruments are shown in the right panel. For a derivation of Cl_y, see Sect. 4.3.

$$Cl_y(\mathrm{MLS}) = \mathrm{HCl}(\mathrm{MLS}) + \mathrm{ClO}(\mathrm{MLS}) + ClONO_2(\mathrm{ACE-FTS}) \quad (2)$$

$$Cl_y(\mathrm{ACE-FTS}) = \mathrm{HCl}(\mathrm{ACE-FTS}) + ClONO_2(\mathrm{ACE-FTS}). \quad (3)$$

For ClO, values during daytime (SZAs less than 85°) are used (Fig. 4). $ClONO_2$ values for the LSTs of SMILES and MLS observations would be needed for a precise calculation of Cl_y. Since the $ClONO_2$ values measured by ACE-FTS at sunrise are higher than they would be during daytime, adding the ACE-FTS $ClONO_2$ value to the sum of ClO and HCl values for SMILES or MLS results in an overestimate of Cl_y values. Conversely, for ACE-FTS, we just take the sum of the HCl and $ClONO_2$ values, because ClO values at sunrise (SZA of 90°) are expected to be small (less than 0.05 ppbv, as was mentioned in Sect. 4.2). However, this results in a slight underestimate of the ACE-FTS Cl_y values, especially above 600 K. Considering these two opposite directions, the HCl/Cl_y ratio difference between ACE-FTS and others above 600 K in the right panel of Fig. 5 can be partly explained. In addition, the vertical shape of the composite Cl_y values is consistent with deduced Cl_y values from N_2O measurements made by MLS and ACE-FTS (see Appendix A).

Although the contribution of HOCl to Cl_y should be discussed, the data quality of this version of HOCl has not been thoroughly evaluated. Thus, we do not address the diurnal cycle of HOCl here. More importantly, since nitrogen dioxide (NO_2) measured by ACE-FTS revealed a value of 2.7 ppbv on average in the 675–700 K bin, ClO observed in daytime could be converted to $ClONO_2$ during sunset. As mentioned in Sect. 4.2, the nighttime value of ClO was also almost zero. Therefore, the diurnal cycle of ClO from zero (nighttime) to 0.35 ppbv (14 LST) in the 675–700 K bin (26 km) is likely mainly caused by the photolysis of $ClONO_2$.

In addition, we further analyzed $ClONO_2$ data taken by MIPAS, as given in Sect. 2.4. The data were extracted for latitudes between 60° S and 66° S and longitudes between 60° W and 120° W, which correspond to the vortex interior during the period of 19–24 November 2009. Since the MIPAS measurements occurred at both day (09:48 LST) and night (22:30 LST) times, the diurnal change in $ClONO_2$ can be seen. For instance, the average and its one sigma standard deviation was 0.91 ± 0.07 ppbv (averaged over 11 data points) for the daytime and 1.13 ± 0.14 ppbv (averaged over 10 data points) for the nighttime in the 675–700 K PT bin. The difference of 0.22 ppbv is comparable to the value of SMILES ClO (0.21 ppbv) in the same PT bin, supporting the conclusion that the diurnal cycle of ClO is caused by the photolysis of $ClONO_2$.

Generally, the HCl/Cl_y ratios are in good agreement among the three sensors for all PT levels between 400 K and 700 K. Taking the average of the four HCl/Cl_y profiles shown in Fig. 5, the difference (X – average) with regard to the average ranges from −5 % in the 650–675 K bin for SMILES-NICT to 8 % in the 625–675 K bins for ACE-FTS, where X is one of SMILES-JAXA, SMILES-NICT, MLS, and ACE-FTS. As mentioned above, the Cl_y value calculated from Eqs. (1) and (2) may have a positive bias up to ∼ 0.2 ppbv, amounting to ∼ 6 % for a Cl_y value of 3.2 ppbv. The HCl/Cl_y ratio is 0.91–0.95 in the peak HCl PT levels (450–500 K) from the three sensors. This strongly suggests that even in the late November period HCl dominates Cl_y inside the Antarctic vortex in the lower stratosphere. The result is consistent with the previous observations in November from the different sensors (Rinsland et al., 1996; Michelsen et al., 1999; Hayashida and Sugita, 2007) and the Aura MLS alone (de Laat and van Weele, 2011). The lower values of ClO in those PT levels also confirm that it was deactivated to reform HCl through the Reactions (R1) to (R4). The data quality of SMILES HCl in the lower stratosphere is sufficient to capture this high HCl/Cl_y ratio phenomenon.

5 Conclusions

SMILES measured several chemical species in the middle atmosphere between October 2009 and April 2010. It was on board the ISS/JEM platform and successfully measured the low-noise emission spectra. We focus on HCl and ClO measured inside the late spring Antarctic vortex on 19–24 November 2009. The data are sorted by EqL fields with the aid of DMPs, and data inside the vortex are averaged. To

confirm the quality of SMILES-JAXA and SMILES-NICT data products from the view point of partitioning of Cl_y, comparisons are made with Aura MLS and ACE-FTS satellite data taken in the same time period.

The SMILES HCl reveals 2.8–3.1 ppbv between 450 K and 500 K, along with a result that the NICT product is, at the maximum, 0.5 ppbv larger than the JAXA product between 425 K and 575 K. The SMILES-NICT HCl agrees within 10 % with the MLS HCl between 450 and 575 K and with the ACE-FTS HCl between 425 and 575 K. Above 575 K, the SMILES-NICT HCl values are, however, 11–19 % smaller than those from MLS and 16–22 % smaller than those from ACE-FTS. The SMILES-JAXA HCl is 10 to 20 % smaller than that from MLS between 400 and 700 K and ACE-FTS between 500 and 700 K.

For ClO in daytime (SZAs less than 85°), SMILES-JAXA and SMILES-NICT agree to within ± 0.05 ppbv between 450 K and 625 K, although the difference between the two products amounts to -0.07 ppbv at 625–675 K and 0.07 ppbv at 425 K. The difference between MLS and SMILES-JAXA or SMILES-NICT was less than ± 0.05 ppbv between 500 K and 650 K with ClO values less than 0.2 ppbv.

Considering the low $ClONO_2$ values also inside the Antarctic vortex as measured by ACE-FTS, HCl was the main component of Cl_y below the 500 K level in November 2009. All three sensors show high values (> 0.9) of the HCl / Cl_y ratios, in agreement with the past observations inside the spring Antarctic vortex. These results can be useful for assessing the performance of recent chemistry–climate models (CCM) in CCM validation activities (e.g., Fig. 6.32 of SPARC CCMVal, 2010). The results from SMILES-JAXA (v2.1) and SMILES-NICT (v2.1.5) suggest the validity of both HCl and ClO data in the lower stratosphere, where HCl values were as high as 3 ppbv during the period studied here.

Appendix A

Comparison between Cl_y and Cl_y*

The composite Cl_y values are compared with a surrogate for Cl_y, which is referred to as Cl_y*. Figure A1 shows vertical profiles of N_2O measured by Aura MLS and ACE-FTS (left panel). The right panel of Fig. A1 shows the Cl_y values from SMILES, MLS, and ACE-FTS (see Sect. 4.3) and the Cl_y* values. The Cl_y* values are deduced from the N_2O data from MLS and ACE-FTS and a polynomial expression between Cl_y* and N_2O (Wetzel et al., 2010). This expression is based on in situ balloon observations of N_2O and several organic chlorine species (Engel et al., 2006), and is calculated for the Arctic stratosphere for mean age of air less than 6 years (Engel et al., 2002). The retrieval method and validation results for MLS and ACE-FTS N_2O measurements are described in Lambert et al. (2007) and Strong et al. (2008), respectively. Precision and accuracy of the MLS version 3.3 N_2O data are

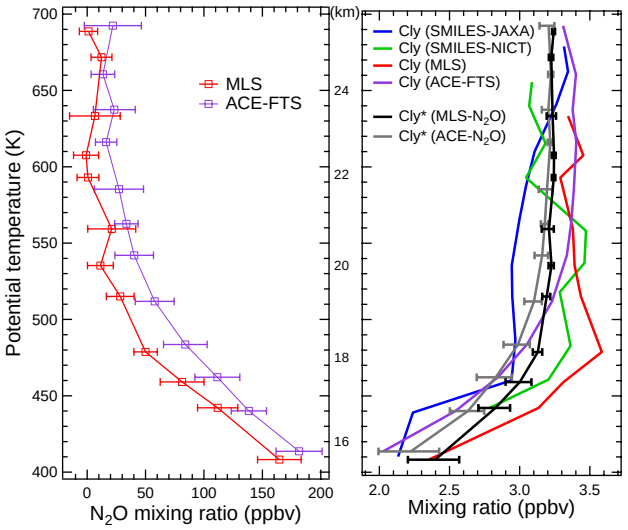

Fig. A1. Vertical profiles of N_2O measured by MLS (red) and ACE-FTS (purple) on 19–24 November 2009 inside the Antarctic vortex (within the edge center) as a function of potential temperature, PT (left panel). The average and $\pm 1\sigma$ standard deviation in each 25 K PT bin are shown. Approximate altitudes corresponding to PT are shown on the right-hand side of the panel. Composite Cl_y values calculated from SMILES, MLS, and ACE-FTS (see Sect. 4.3) and the Cl_y* values deduced from the N_2O values from MLS and ACE-FTS (see Appendix A) are shown in the right panel. Bars show corresponding Cl_y* values estimated from the standard deviations of N_2O data.

estimated to be 8–9 % and 13–25 %, respectively, for 46.4–100 hPa levels (Livesey et al., 2011). Fitting errors for the ACE-FTS version 2.2 N_2O data are estimated to be 4 % for 5–35 km (Strong et al., 2008).

The Cl_y* values calculated from the expression are then decreased to the year 2009 as was done in Wetzel et al. (2012), since the expression is valid for the years 2000–2003. It should be noted that recent satellite measurements of SF_6 from the Michelson Interferometer for Passive Atmospheric Sounding (MIPAS) on board Envisat suggested an inter-hemispheric difference in "apparent age" of air inside the Arctic and Antarctic vortices (Stiller et al., 2008, 2012). For N_2O data less than 20–30 ppbv (above ~ 500 K), they could be influenced by intrusions of mesospheric air into the Antarctic vortex. The real age of air in the Antarctic vortex might be different from that in the Arctic, making the Cl_y* values estimated uncertain. Thus, the Cl_y* values presented here are solely reference values.

Absolute differences between MLS and ACE-FTS N_2O data amount to 30 ppbv. It could be partly due to a different degree of descent of air. Such differences reflect the Cl_y* values; those from MLS are larger than those from ACE-FTS below 500 K levels. The Cl_y and Cl_y* values from ACE-FTS (purple and gray lines) agree well below 500 K levels. The result presented here provides some sort of uncertainty range

for the Cl_y level in the Antarctic stratosphere in this time period.

Acknowledgements. The JEM/SMILES mission is a joint project of the Japan Aerospace Exploration Agency (JAXA) and the National Institute of Information and Communications Technology (NICT). We thank the JEM/SMILES mission team and the related members before the mission. Work at the Jet Propulsion Laboratory (JPL), California Institute of Technology, was done under contract with the National Aeronautics and Space Administration (NASA). The Atmospheric Chemistry Experiment (ACE), also known as SCISAT-1, is a Canadian-led mission mainly supported by the Canadian Space Agency (CSA) and the Natural Sciences and Engineering Research Council (NSERC) of Canada. The joint IMK/IAA generated MIPAS/Envisat data were obtained from the IMK – Atmospheric Trace Gases and Remote Sensing (ASF) data server (http://www.imk-asf.kit.edu/english/308.php). Instructions on using the MIPAS data from Thomas von Clarmann are acknowledged. Helpful comments from Rolf Müller are also acknowledged. This work was partly done by using resources of the OneSpaceNet in the NICT Science Cloud. This work was performed as one of approved themes under the JEM/SMILES Research Announcement.

Edited by: H. Worden

References

Baron, P., Urban, J., Sagawa, H., Möller, J., Murtagh, D. P., Mendrok, J., Dupuy, E., Sato, T. O., Ochiai, S., Suzuki, K., Manabe, T., Nishibori, T., Kikuchi, K., Sato, R., Takayanagi, M., Murayama, Y., Shiotani, M., and Kasai, Y.: The Level 2 research product algorithms for the Superconducting Submillimeter-Wave Limb-Emission Sounder (SMILES), Atmos. Meas. Tech., 4, 2105–2124, doi:10.5194/amt-4-2105-2011, 2011.

Bernath, P. F., McElroy, C. T., Abrams, M. C., Boone, C. D., Butler, M., Camy-Peyret, C., Carleer, M., Clerbaux, C., Coheur, P.-F., Colin, R., DeCola, P., DeMaziére, M., Drummond, J. R., Dufour, D., Evans, W. F. J., Fast, H., Fussen, D., Gilbert, K., Jennings, D. E., Llewellyn, E. J., Lowe, R. P., Mahieu, E., McConnell, J. C., McHugh, M., McLeod, S. D., Michaud, R., Midwinter, C., Nassar, R., Nichitiu, F., Nowlan, C., Rinsland, C. P., Rochon, Y. J., Rowlands, N., Semeniuk, K., Simon, P., Skelton, R., Sloan, J. J., Soucy, M.-A., Strong, K., Tremblay, P., Turnbull, D., Walker, K. A., Walkty, I., Wardle, D. A., Wehrle, V., Zander, R., and Zou, J.: Atmospheric Chemistry Experiment (ACE): Mission overview, Geophys. Res. Lett., 32, L15S01, doi:10.1029/2005GL022386, 2005.

Bonne, G. P., Stimpfle, R. M., Cohen, R. C., Voss, P. B., Perkins, K. K., Anderson, J. G., Salawitch, R. J., Elkins, J. W., Dutton, G. S., Jucks, K. W., and Toon, G. C.: An examination of the inorganic chlorine budget in the lower stratosphere, J. Geophys. Res., 105, 1957–1971, doi:10.1029/1999JD900996, 2000.

Boone, C. D., Nassar, R., Walker, K. A., Rochon, Y., McLeod, S. D., Rinsland, C. P., and Bernath, P. F.: Retrievals for the atmospheric chemistry experiment Fourier-transform spectrometer, Appl. Opt., 44, 7218–7231, doi:10.1364/AO.44.007218, 2005.

Brenninkmeijer, C. A. M., Müller, R., Crutzen, P. J., Lowe, D. C., Manning, M. R., Sparks, R. J., and van Velthoven, P. F. J.: A large ^{13}CO deficit in the lower Antarctic stratosphere due to "Ozone Hole" Chemistry: Part I, Observations, Geophys. Res. Lett., 23, 2125–2128, doi:10.1029/96GL01471, 1996.

Butchart, N. and Remsberg, E. E.: The area of the stratospheric polar vortex as a diagnostic for tracer transport on an isentropic surface, J. Atmos. Sci., 43, 1319–1339, 1986.

Cazzoli, G. and Puzzarini, C.: Hyperfine structure of the $J = 1 \leftarrow 0$ transition of $H^{35}Cl$ and $H^{37}Cl$: improved ground state parameters, J. Mol. Spectrosc., 226, 161–168, doi:10.1016/j.jms.2004.03.020, 2004.

Ceccherini, S., Carli, B., Pascale, E., Prosperi, M., Raspollini, P., and Dinelli, B. M.: Comparison of measurements made with two different instruments of the same atmospheric vertical profile, Appl. Opt., 42, 6465–6473, doi:10.1364/AO.42.006465, 2003.

Chipperfield, M. P., Santee, M. L., Froidevaux, L., Manney, G. L., Read, W. G., Waters, J. W., Roche, A. E., and Russell, J. M.: Analysis of UARS data in the southern polar vortex in September 1992 using a chemical transport model, J. Geophys. Res., 101, 18861–18881, doi:10.1029/96JD00936, 1996.

Cofield, R. and Stek, P.: Design and field-of-view calibration of 114-660-GHz optics of the Earth observing system microwave limb sounder, Geoscience and Remote Sensing, IEEE Transactions on, 44, 1166–1181, doi:10.1109/TGRS.2006.873234, 2006.

de Laat, A. T. J. and van Weele, M.: The 2010 Antarctic ozone hole: Observed reduction in ozone destruction by minor sudden stratospheric warmings, Sci. Rep., 1, 1–8, doi:10.1038/srep00038, 2011.

de Laat, A. T. J., van der A, R. J., Allaart, M. A. F., van Weele, M., Benitez, G. C., Casiccia, C., Paes Leme, N. M., Quel, E., Salvador, J., and Wolfram, E.: Extreme sunbathing: Three weeks of small total O_3 columns and high UV radiation over the southern tip of South America during the 2009 Antarctic O_3 hole season, Geophys. Res. Lett., 37, L14805, doi:10.1029/2010GL043699, 2010.

Douglass, A. R. and Kawa, S. R.: Contrast between 1992 and 1997 high-latitude spring Halogen Occultation Experiment observations of lower stratospheric HCl, J. Geophys. Res., 104, 18739–18754, doi:10.1029/1999JD900281, 1999.

Douglass, A. R., Schoeberl, M. R., Stolarski, R. S., Waters, J. W., Russell, J. M., Roche, A. E., and Massie, S. T.: Interhemispheric differences in springtime production of HCl and $ClONO_2$ in the polar vortices, J. Geophys. Res., 100, 13967–13978, doi:10.1029/95JD00698, 1995.

Dufour, G., Nassar, R., Boone, C. D., Skelton, R., Walker, K. A., Bernath, P. F., Rinsland, C. P., Semeniuk, K., Jin, J. J., McConnell, J. C., and Manney, G. L.: Partitioning between the inorganic chlorine reservoirs HCl and $ClONO_2$ during the Arctic winter 2005 from the ACE-FTS, Atmos. Chem. Phys., 6, 2355–2366, doi:10.5194/acp-6-2355-2006, 2006.

Engel, A., Strunk, M., Müller, M., Haase, H.-P., Poss, C., Levin, I., and Schmidt, U.: Temporal development of total chlorine in the high-latitude stratosphere based on reference distributions of mean age derived from CO_2 and SF_6, J. Geophys. Res., 107, ACH 1–1–ACH 1–11, doi:10.1029/2001JD000584, 2002.

Engel, A., Möbius, T., Haase, H.-P., Bönisch, H., Wetter, T., Schmidt, U., Levin, I., Reddmann, T., Oelhaf, H., Wetzel, G.,

Grunow, K., Huret, N., and Pirre, M.: Observation of mesospheric air inside the arctic stratospheric polar vortex in early 2003, Atmos. Chem. Phys., 6, 267–282, doi:10.5194/acp-6-267-2006, 2006.

Fischer, H., Birk, M., Blom, C., Carli, B., Carlotti, M., von Clarmann, T., Delbouille, L., Dudhia, A., Ehhalt, D., Endemann, M., Flaud, J. M., Gessner, R., Kleinert, A., Koopman, R., Langen, J., López-Puertas, M., Mosner, P., Nett, H., Oelhaf, H., Perron, G., Remedios, J., Ridolfi, M., Stiller, G., and Zander, R.: MIPAS: an instrument for atmospheric and climate research, Atmos. Chem. Phys., 8, 2151–2188, doi:10.5194/acp-8-2151-2008, 2008.

Grooß, J.-U., Pierce, R. B., Crutzen, P. J., Grose, W. L., and Russell, J. M.: Re-formation of chlorine reservoirs in southern hemisphere polar spring, J. Geophys. Res., 102, 13141–13152, doi:10.1029/96JD03505, 1997.

Grooß, J.-U., Paul, K., and Müller, R.: Ozone chemistry during the 2002 Antarctic vortex split, J. Atmos. Sci., 62, 860–870, doi:10.1175/JAS-3330.1, 2005.

Grooß, J.-U., Brautzsch, K., Pommrich, R., Solomon, S., and Müller, R.: Stratospheric ozone chemistry in the Antarctic: what determines the lowest ozone values reached and their recovery?, Atmos. Chem. Phys., 11, 12217–12226, doi:10.5194/acp-11-12217-2011, 2011.

Harrison, J. J. and Bernath, P. F.: ACE-FTS observations of acetonitrile in the lower stratosphere, Atmos. Chem. Phys., 13, 7405–7413, doi:10.5194/acp-13-7405-2013, 2013.

Hayashida, S. and Sugita, T.: Hemispheric contrast of inorganic chlorine Partitioning in the polar lower stratosphere during ozone recovery period observed from space, Sci. Online Lett. Atmos., 3, 117–120, doi:10.2151/sola.2007-030, 2007.

Höpfner, M., von Clarmann, T., Fischer, H., Glatthor, N., Grabowski, U., Kellmann, S., Kiefer, M., Linden, A., Mengistu Tsidu, G., Milz, M., Steck, T., Stiller, G. P., Wang, D. Y., and Funke, B.: First spaceborne observations of Antarctic stratospheric $ClONO_2$ recovery: Austral spring 2002, J. Geophys. Res., 109, D11308, doi:10.1029/2004JD004609, 2004.

Jaeglé, L., Webster, C. R., May, R. D., Scott, D. C., Stimpfle, R. M., Kohn, D. W., Wennberg, P. O., Hanisco, T. F., Cohen, R. C., Proffitt, M. H., Kelly, K. K., Elkins, J., Baumgardner, D., Dye, J. E., Wilson, J. C., Pueschel, R. F., Chan, K. R., Salawitch, R. J., Tuck, A. F., Hovde, S. J., and Yung, Y. L.: Evolution and stoichiometry of heterogeneous processing in the Antarctic stratosphere, J. Geophys. Res., 102, 13235–13253, doi:10.1029/97JD00935, 1997.

Kasai, Y., Sagawa, H., Kreyling, D., Dupuy, E., Baron, P., Mendrok, J., Suzuki, K., Sato, T. O., Nishibori, T., Mizobuchi, S., Kikuchi, K., Manabe, T., Ozeki, H., Sugita, T., Fujiwara, M., Irimajiri, Y., Walker, K. A., Bernath, P. F., Boone, C., Stiller, G., von Clarmann, T., Orphal, J., Urban, J., Murtagh, D., Llewellyn, E. J., Degenstein, D., Bourassa, A. E., Lloyd, N. D., Froidevaux, L., Birk, M., Wagner, G., Schreier, F., Xu, J., Vogt, P., Trautmann, T., and Yasui, M.: Validation of stratospheric and mesospheric ozone observed by SMILES from International Space Station, Atmos. Meas. Tech., 6, 2311–2338, doi:10.5194/amt-6-2311-2013, 2013.

Kikuchi, K., Nishibori, T., Ochiai, S., Ozeki, H., Irimajiri, Y., Kasai, Y., Koike, M., Manabe, T., Mizukoshi, K., Murayama, Y., Nagahama, T., Sano, T., Sato, R., Seta, M., Takahashi, C., Takayanagi, M., Masuko, H., Inatani, J., Suzuki, M., and Shiotani, M.: Overview and early results of the Superconducting Submillimeter-Wave Limb-Emission Sounder (SMILES), J. Geophys. Res., 115, D23306, doi:10.1029/2010JD014379, 2010.

Konopka, P., Grooß, J.-U., Bausch, S., Müller, R., McKenna, D. S., Morgenstern, O., and Orsolini, Y.: Dynamics and chemistry of vortex remnants in late Arctic spring 1997 and 2000: Simulations with the Chemical Lagrangian Model of the Stratosphere (CLaMS), Atmos. Chem. Phys., 3, 839–849, doi:10.5194/acp-3-839-2003, 2003.

Kreher, K., Keys, J. G., Johnston, P. V., Platt, U., and Liu, X.: Ground-based measurements of OClO and HCl in austral spring 1993 at Arrival Heights, Antarctica, Geophys. Res. Lett., 23, 1545–1548, doi:10.1029/96GL01318, 1996.

Lambert, A., Read, W. G., Livesey, N. J., Santee, M. L., Manney, G. L., Froidevaux, L., Wu, D. L., Schwartz, M. J., Pumphrey, H. C., Jimenez, C., Nedoluha, G. E., Cofield, R. E., Cuddy, D. T., Daffer, W. H., Drouin, B. J., Fuller, R. A., Jarnot, R. F., Knosp, B. W., Pickett, H. M., Perun, V. S., Snyder, W. V., Stek, P. C., Thurstans, R. P., Wagner, P. A., Waters, J. W., Jucks, K. W., Toon, G. C., Stachnik, R. A., Bernath, P. F., Boone, C. D., Walker, K. A., Urban, J., Murtagh, D., Elkins, J. W., and Atlas, E.: Validation of the Aura Microwave Limb Sounder middle atmosphere water vapor and nitrous oxide measurements, J. Geophys. Res., 112, D24S36, doi:10.1029/2007JD008724, 2007.

Lambert, A., Santee, M. L., Wu, D. L., and Chae, J. H.: A-train CALIOP and MLS observations of early winter Antarctic polar stratospheric clouds and nitric acid in 2008, Atmos. Chem. Phys., 12, 2899–2931, doi:10.5194/acp-12-2899-2012, 2012.

Liebe, H. J., Hufford, G. A., and Cotton, M. G. (Eds.): Propagation modeling of moist air and suspended water/ice particles at frequencies below 1000 GHz, 52nd Specialists Meeting of the Electromagnetic Wave Propagation Panel, Palma De Mallorca, Spain, 1993.

Lingenfelser, G. S. and Grose, W. L.: Use of long-lived tracer observations to examine transport characteristics in the lower stratosphere, J. Geophys. Res., 107, ACL 6-1–ACL 6-13, doi:10.1029/2001JD001296, 2002.

Liu, X., Blatherwick, R. D., Murcray, F. J., Keys, J. G., and Solomon, S.: Measurements and model calculations of HCl column amounts and related parameters over McMurdo during the austral spring in 1989, J. Geophys. Res., 97, 20795–20804, doi:10.1029/92JD02435, 1992.

Livesey, N., Van Snyder, W., Read, W., and Wagner, P.: Retrieval algorithms for the EOS Microwave Limb Sounder (MLS), Geoscience and Remote Sensing, IEEE Transactions on, 44, 1144–1155, doi:10.1109/TGRS.2006.872327, 2006.

Livesey, N. J., Read, W. G., Froidevaux, L., Lambert, A., Manney, G. L., Pumphrey, H. C., Santee, M. L., Schwartz, M. J., Wang, S., Cofield, R. E., Cuddy, D. T., Fuller, R. A., Jarnot, R. F., Jiang, J. H., Knosp, B. W., Stek, P. C., Wagner, P. A., and Wu, D. L.: Earth Observing System (EOS), Aura Microwave Limb Sounder (MLS), Version 3.3 Level 2 data quality and description document, D-33509, Jet Propulsion Laboratory, California Institute of Technology, Pasadena, California, 2011.

Mahieu, E., Duchatelet, P., Demoulin, P., Walker, K. A., Dupuy, E., Froidevaux, L., Randall, C., Catoire, V., Strong, K., Boone, C. D., Bernath, P. F., Blavier, J.-F., Blumenstock, T., Coffey, M., De Mazière, M., Griffith, D., Hannigan, J., Hase, F., Jones, N., Jucks, K. W., Kagawa, A., Kasai, Y., Mebarki, Y., Mikuteit, S., Nassar,

R., Notholt, J., Rinsland, C. P., Robert, C., Schrems, O., Senten, C., Smale, D., Taylor, J., Tétard, C., Toon, G. C., Warneke, T., Wood, S. W., Zander, R., and Servais, C.: Validation of ACE-FTS v2.2 measurements of HCl, HF, CCl_3F and CCl_2F_2 using space-, balloon- and ground-based instrument observations, Atmos. Chem. Phys., 8, 6199–6221, doi:10.5194/acp-8-6199-2008, 2008.

Manney, G. L., Daffer, W. H., Zawodny, J. M., Bernath, P. F., Hoppel, K. W., Walker, K. A., Knosp, B. W., Boone, C., Remsberg, E. E., Santee, M. L., Harvey, V. L., Pawson, S., Jackson, D. R., Deaver, L., McElroy, C. T., McLinden, C. A., Drummond, J. R., Pumphrey, H. C., Lambert, A., Schwartz, M. J., Froidevaux, L., McLeod, S., Takacs, L. L., Suarez, M. J., Trepte, C. R., Cuddy, D. C., Livesey, N. J., Harwood, R. S., and Waters, J. W.: Solar occultation satellite data and derived meteorological products: Sampling issues and comparisons with Aura Microwave Limb Sounder, J. Geophys. Res., 112, D24S50, doi:10.1029/2007JD008709, 2007.

Manney, G. L., Santee, M. L., Rex, M., Livesey, N. J., Pitts, M. C., Veefkind, P., Nash, E. R., Wohltmann, I., Lehmann, R., Froidevaux, L., Poole, L. R., Schoeberl, M. R., Haffner, D. P., Davies, J., Dorokhov, V., Gernandt, H., Johnson, B., Kivi, R., Kyrö, E., Larsen, N., Levelt, P. F., Makshtas, A., McElroy, C. T., Nakajima, H., Parrondo, M. C., Tarasick, D. W., von der Gathen, P., Walker, K. A., and Zinoviev, N. S.: Unprecedented Arctic ozone loss in 2011, Nature, 478, 469–475, doi:10.1038/nature10556, 2011.

Michelsen, H. A., Webster, C. R., Manney, G. L., Scott, D. C., Margitan, J. J., May, R. D., Irion, F. W., Gunson, M. R., Russell, J. M., and Spivakovsky, C. M.: Maintenance of high HCl/Cl_y and NOx/NOy in the Antarctic vortex: A chemical signature of confinement during spring, J. Geophys. Res., 104, 26419–26436, doi:10.1029/1999JD900473, 1999.

Mickley, L. J., Abbatt, J. P. D., Frederick, J. E., and Russell, J. M.: Evolution of chlorine and nitrogen species in the lower stratosphere during Antarctic spring: Use of tracers to determine chemical change, J. Geophys. Res., 102, 21479–21491, doi:10.1029/97JD00422, 1997.

Mitsuda, C., Suzuki, M., Iwata, Y., Manago, N., Naito, Y., Takahashi, C., Imai, K., Nishimoto, E., Hayashi, H., Shiotani, M., Sano, T., Takayanagi, M., and Taniguchi, H.: Current status of level 2 product of Superconducting Submillimeter-Wave Limb-Emission Sounder (SMILES), in: Sensors, Systems, and Next-generation Satellites XV, edited by: Meynart, R., Neeck, S. P., and Shimoda, H., vol. 8176 of Proc. SPIE, doi:10.1117/12.898135, 81760M, 2011.

Müller, R., Brenninkmeijer, C. A. M., and Crutzen, P. J.: A Large ^{13}CO deficit in the lower Antarctic stratosphere due to "ozone hole" chemistry: Part II, Modeling, Geophys. Res. Lett., 23, 2129–2132, doi:10.1029/96GL01472, 1996.

Murcray, F. J., Goldman, A., Blatherwick, R., Matthews, A., and Jones, N.: HNO_3 and HCl amounts over McMurdo during the spring of 1987, J. Geophys. Res., 94, 16615–16618, doi:10.1029/JD094iD14p16615, 1989.

Murtagh, D., Frisk, U., Merino, F., Ridal, M., Jonsson, A., Stegman, J., Witt, G., Eriksson, P., Jiménez, C., Megie, G., de La Noë, J., Ricaud, P., Baron, P., Pardo, J. R., Hauchcorne, A., Llewellyn, E. J., Degenstein, D. A., Gattinger, R. L., Lloyd, N. D., Evans, W. F. J., McDade, I. C., Haley, C. S., Sioris, C., von Savigny, C., Solheim, B. H., McConnell, J. C., Strong, K., Richardson, E. H., Leppelmeier, G. W., Kyrölä, E., Auvinen, H., and Oikarinen, L.: An overview of the Odin atmospheric mission, Can. J. Phys., 80, 309–319, doi:10.1139/p01-157, 2002.

NOAA: Southern Hemisphere Winter 2009 Summary, Stratosphere: Winter bulletins, http://www.cpc.ncep.noaa.gov/products/stratosphere/winter_bulletins/, 2009.

Oh, J. and Cohen, E.: Pressure broadening of ClO by N_2 and O_2 near 204 and 649 GHz and new frequency measurements between 632 and 725 GHz, J. Quant. Spectrosc. Radiat. Transfer, 52, 151–156, doi:10.1016/0022-4073(94)90004-3, 1994.

Pardo, J., Cernicharo, J., and Serabyn, E.: Atmospheric transmission at microwaves (ATM): an improved model for millimeter/submillimeter applications, Antennas and Propagation, IEEE Transactions on, 49, 1683–1694, doi:10.1109/8.982447, 2001.

Perrin, A., Puzzarini, C., Colmont, J.-M., Verdes, C., Wlodarczak, G., Cazzoli, G., Buehler, S., Flaud, J.-M., and Demaison, J.: Molecular Line Parameters for the "MASTER" (Millimeter Wave Acquisitions for Stratosphere/Troposphere Exchange Research) Database, J. Atmos. Chem., 51, 161–205, doi:10.1007/s10874-005-7185-9, 2005.

Prather, M. and Jaffe, A. H.: Global impact of the Antarctic ozone hole: Chemical propagation, J. Geophys. Res., 95, 3473–3492, doi:10.1029/JD095iD04p03473, 1990.

Read, W. G., Shippony, Z., and Snyder, W. V.: Earth Observing System (EOS), Aura Microwave Limb Sounder (MLS), forward model algorithm theoretical basis document, Version 1.0, D-18130, Jet Propulsion Laboratory, California Institute of Technology, Pasadena, California, 2004.

Reinecker, M. M., Suarez, M. J., Todling, R., Bacmeister, J., Takacs, L., Liu, H.-C., Gu, W., Sienkiewicz, M., Koster, R. D., Gelaro, R., Stajner, I., and Nielsen, J. E.: The GEOS-5 data assimilation system: Documentations of versions of 5.0.1, 5.1.0, and 5.2.0, vol. 27 of Technical Report Series on Global Modeling and Data Assimilation, NASA/TM-2008-104606, Hanover, MD, 2008.

Ridolfi, M., Ceccherini, S., and Carli, B.: Optimal interpolation method for intercomparison of atmospheric measurements, Opt. Lett., 31, 855–857, doi:10.1364/OL.31.000855, 2006.

Rinsland, C. P., Gunson, M. R., Salawitch, R. J., Michelsen, H. A., Zander, R., Newchurch, M. J., Abbas, M. M., Abrams, M. C., Manney, G. L., Chang, A. Y., Irion, F. W., Goldman, A., and Mahieu, E.: ATMOS/ATLAS-3 measurements of stratospheric chlorine and reactive nitrogen partitioning inside and outside the November 1994 Antarctic vortex, Geophys. Res. Lett., 23, 2365–2368, doi:10.1029/96GL01474, 1996.

Rodgers, C. D.: Inverse methods for atmospheric sounding: Theory and practice, vol. 2 of Series on Atmospheric, Oceanic and Planetary physics, World Scientific Publishing, London, 238 pp., 2000.

Sagawa, H., Sato, T. O., Baron, P., Dupuy, E., Livesey, N., Urban, J., von Clarmann, T., de Lange, A., Wetzel, G., Kagawa, A., Murtagh, D., and Kasai, Y.: Comparison of SMILES ClO profiles with other satellite and balloon-based measurements, Atmos. Meas. Tech. Discuss., 6, 613–663, doi:10.5194/amtd-6-613-2013, 2013.

Santee, M. L., Froidevaux, L., Manney, G. L., Read, W. G., Waters, J. W., Chipperfield, M. P., Roche, A. E., Kumer, J. B., Mergenthaler, J. L., and Russell, J. M.: Chlorine deactivation in the lower stratospheric polar regions during late win-

ter: Results from UARS, J. Geophys. Res., 101, 18835–18859, doi:10.1029/96JD00580, 1996.

Santee, M. L., Lambert, A., Read, W. G., Livesey, N. J., Manney, G. L., Cofield, R. E., Cuddy, D. T., Daffer, W. H., Drouin, B. J., Froidevaux, L., Fuller, R. A., Jarnot, R. F., Knosp, B. W., Perun, V. S., Snyder, W. V., Stek, P. C., Thurstans, R. P., Wagner, P. A., Waters, J. W., Connor, B., Urban, J., Murtagh, D., Ricaud, P., Barret, B., Kleinböhl, A., Kuttippurath, J., Küllmann, H., von Hobe, M., Toon, G. C., and Stachnik, R. A.: Validation of the Aura Microwave Limb Sounder ClO measurements, J. Geophys. Res., 113, D15S22, doi:10.1029/2007JD008762, 2008a.

Santee, M. L., MacKenzie, I. A., Manney, G. L., P., C. M., Bernath, P. F., Walker, K. A., Boone, C. D., Froidevaux, L., Livesey, N. J., and Waters, J. W.: A study of stratospheric chlorine partitioning based on new satellite measurements and modeling, J. Geophys. Res., 113, D12307, doi:10.1029/2007JD009057, 2008b.

Santee, M. L., Manney, G. L., Livesey, N. J., Froidevaux, L., Schwartz, M. J., and Read, W. G.: Trace gas evolution in the lowermost stratosphere from Aura Microwave Limb Sounder measurements, J. Geophys. Res., 116, D18306, doi:10.1029/2011JD015590, 2011.

Sato, T. O., Sagawa, H., Kreyling, D., Manabe, T., Ochiai, S., Kikuchi, K., Baron, P., Mendrok, J., Urban, J., Murtagh, D., Yasui, M., and Kasai, Y.: Strato-mesospheric ClO observations by SMILES: error analysis and diurnal variation, Atmos. Meas. Tech., 5, 2809–2825, doi:10.5194/amt-5-2809-2012, 2012.

Shiotani, M., Takayanagi, M., Suzuki, M., and Sano, T.: Recent results from the Superconducting submillimeter-wave limb-emission sounder (SMILES) onboard ISS/JEM, in: Sensors, Systems, and Next-generation Satellites XIV, edited by: Meynart, R., Neeck, S. P., and Shimoda, H., vol. 7826 of Proc. SPIE, doi:10.1117/12.865806, 78260D, 2010.

SPARC CCMVal: SPARC Report on the Evaluation of Chemistry-Climate Models, edited by: Eyring, V., Shepherd, T. G., and Waugh, D. W., SPARC Report No. 5, WCRP-132, WMO/TD-No. 1526, 434 pp., http://www.sparc-climate.org/, 2010.

Stachnik, R. A., Millán, L., Jarnot, R., Monroe, R., McLinden, C., Kühl, S., Pukite, J., Shiotani, M., Suzuki, M., Kasai, Y., Goutail, F., Pommereau, J. P., Dorf, M., and Pfeilsticker, K.: Stratospheric BrO abundance measured by a balloon-borne submillimeterwave radiometer, Atmos. Chem. Phys., 13, 3307–3319, doi:10.5194/acp-13-3307-2013, 2013.

Stiller, G. P., von Clarmann, T., Höpfner, M., Glatthor, N., Grabowski, U., Kellmann, S., Kleinert, A., Linden, A., Milz, M., Reddmann, T., Steck, T., Fischer, H., Funke, B., López-Puertas, M., and Engel, A.: Global distribution of mean age of stratospheric air from MIPAS SF_6 measurements, Atmos. Chem. Phys., 8, 677–695, doi:10.5194/acp-8-677-2008, 2008.

Stiller, G. P., von Clarmann, T., Haenel, F., Funke, B., Glatthor, N., Grabowski, U., Kellmann, S., Kiefer, M., Linden, A., Lossow, S., and López-Puertas, M.: Observed temporal evolution of global mean age of stratospheric air for the 2002 to 2010 period, Atmos. Chem. Phys., 12, 3311–3331, doi:10.5194/acp-12-3311-2012, 2012.

Strong, K., Wolff, M. A., Kerzenmacher, T. E., Walker, K. A., Bernath, P. F., Blumenstock, T., Boone, C., Catoire, V., Coffey, M., De Mazière, M., Demoulin, P., Duchatelet, P., Dupuy, E., Hannigan, J., Höpfner, M., Glatthor, N., Griffith, D. W. T., Jin, J. J., Jones, N., Jucks, K., Kuellmann, H., Kuttippurath, J., Lambert, A., Mahieu, E., McConnell, J. C., Mellqvist, J., Mikuteit, S., Murtagh, D. P., Notholt, J., Piccolo, C., Raspollini, P., Ridolfi, M., Robert, C., Schneider, M., Schrems, O., Semeniuk, K., Senten, C., Stiller, G. P., Strandberg, A., Taylor, J., Tétard, C., Toohey, M., Urban, J., Warneke, T., and Wood, S.: Validation of ACE-FTS N_2O measurements, Atmos. Chem. Phys., 8, 4759–4786, doi:10.5194/acp-8-4759-2008, 2008.

Sugita, T., Kasai, Y., Terao, Y., Hayashida, S., Manney, G. L., Daffer, W. H., Sagawa, H., Suzuki, M., and Shiotani, M.: HCl / Cl_y ratios just before the breakup of the Antarctic vortex as observed by SMILES/MLS/ACE-FTS, in: Remote Sensing of Atmosphere, Clouds, and Precipitation IV, edited by: Hayasaka, T., Nakamura, K., and Im, E., vol. 8523 of Proc. SPIE, doi:10.1117/12.975667, 85231K, 2012.

Suzuki, M., Mitsuda, C., Kikuchi, K., Nishibori, T., Ochiai, S., Ozeki, H., Sano, T., Mizobuchi, S., Takahashi, C., Manago, N., Imai, K., Naito, Y., Hayashi, H., Nishimoto, E., and Shiotani, M.: Overview of Superconducting Submillimeter-Wave Limb-Emission sounder (SMILES) and sensitivity to chlorine monoxide, ClO, IEEJ Trans. Fund. Mater., 132, 609–615, doi:10.1541/ieejfms.132.609, 2012.

Takahashi, C., Ochiai, S., and Suzuki, M.: Operational retrieval algorithms for JEM/SMILES level 2 data processing system, J. Quant. Spectrosc. Radiat. Transfer, 111, 160–173, doi:10.1016/j.jqsrt.2009.06.005, 2010.

Tuck, A. F., Brune, W. H., and Hipskind, R. S.: Airborne Southern Hemisphere Ozone Experiment Measurements for Assessing the Effects of Stratospheric Aircraft (ASHOE/MAESA): A road map, J. Geophys. Res., 102, 3901–3904, doi:10.1029/96JD02745, 1997.

von Clarmann, T., Höpfner, M., Kellmann, S., Linden, A., Chauhan, S., Funke, B., Grabowski, U., Glatthor, N., Kiefer, M., Schieferdecker, T., Stiller, G. P., and Versick, S.: Retrieval of temperature, H_2O, O_3, HNO_3, CH_4, N_2O, $ClONO_2$ and ClO from MIPAS reduced resolution nominal mode limb emission measurements, Atmos. Meas. Tech., 2, 159–175, doi:10.5194/amt-2-159-2009, 2009.

von Clarmann, T., Funke, B., López-Puertas, M., Kellmann, S., Linden, A., Stiller, G. P., Jackman, C. H., and Harvey, V. L.: The solar proton events in 2012 as observed by MIPAS, Geophys. Res. Lett., 40, 2339–2343, doi:10.1002/grl.50119, 2013.

Waters, J., Froidevaux, L., Harwood, R., Jarnot, R., Pickett, H., Read, W., Siegel, P., Cofield, R., Filipiak, M., Flower, D., Holden, J., Lau, G., Livesey, N., Manney, G., Pumphrey, H., Santee, M., Wu, D., Cuddy, D., Lay, R., Loo, M., Perun, V., Schwartz, M., Stek, P., Thurstans, R., Boyles, M., Chandra, K., Chavez, M., Chen, G.-S., Chudasama, B., Dodge, R., Fuller, R., Girard, M., Jiang, J., Jiang, Y., Knosp, B., LaBelle, R., Lam, J., Lee, K., Miller, D., Oswald, J., Patel, N., Pukala, D., Quintero, O., Scaff, D., Van Snyder, W., Tope, M., Wagner, P., and Walch, M.: The Earth Observing System Microwave Limb Sounder (EOS MLS) on the Aura satellite, Geoscience and Remote Sensing, IEEE Transactions on, 44, 1075–1092, doi:10.1109/TGRS.2006.873771, 2006.

Wegner, T., Grooß, J.-U., von Hobe, M., Stroh, F., Suminska-Ebersoldt, O., Volk, C. M., Hösen, E., Mitev, V., Shur, G., and Müller, R.: Heterogeneous chlorine activation on stratospheric aerosols and clouds in the Arctic polar vortex, Atmos. Chem. Phys., 12, 11095–11106, doi:10.5194/acp-12-11095-2012, 2012.

Wetzel, G., Oelhaf, H., Kirner, O., Ruhnke, R., Friedl-Vallon, F., Kleinert, A., Maucher, G., Fischer, H., Birk, M., Wagner, G., and Engel, A.: First remote sensing measurements of ClOOCl along with ClO and $ClONO_2$ in activated and deactivated Arctic vortex conditions using new ClOOCl IR absorption cross sections, Atmos. Chem. Phys., 10, 931–945, doi:10.5194/acp-10-931-2010, 2010.

Wetzel, G., Oelhaf, H., Kirner, O., Friedl-Vallon, F., Ruhnke, R., Ebersoldt, A., Kleinert, A., Maucher, G., Nordmeyer, H., and Orphal, J.: Diurnal variations of reactive chlorine and nitrogen oxides observed by MIPAS-B inside the January 2010 Arctic vortex, Atmos. Chem. Phys., 12, 6581–6592, doi:10.5194/acp-12-6581-2012, 2012.

Wilmouth, D. M., Stimpfle, R. M., Anderson, J. G., Elkins, J. W., Hurst, D. F., Salawitch, R. J., and Lait, L. R.: Evolution of inorganic chlorine partitioning in the Arctic polar vortex, J. Geophys. Res., 111, D16308, doi:10.1029/2005JD006951, 2006.

WMO: Scientific Assessment of Ozone Depletion: 2006, Global Ozone Research and Monitoring Project–Report No. 50, 572 pp., Geneva, Switzerland, 2007.

WMO: Scientific Assessment of Ozone Depletion: 2010, Global Ozone Research and Monitoring Project–Report No. 52, 516 pp., Geneva, Switzerland, 2011.

Wolff, M. A., Kerzenmacher, T., Strong, K., Walker, K. A., Toohey, M., Dupuy, E., Bernath, P. F., Boone, C. D., Brohede, S., Catoire, V., von Clarmann, T., Coffey, M., Daffer, W. H., De Mazière, M., Duchatelet, P., Glatthor, N., Griffith, D. W. T., Hannigan, J., Hase, F., Höpfner, M., Huret, N., Jones, N., Jucks, K., Kagawa, A., Kasai, Y., Kramer, I., Küllmann, H., Kuttippurath, J., Mahieu, E., Manney, G., McElroy, C. T., McLinden, C., Mébarki, Y., Mikuteit, S., Murtagh, D., Piccolo, C., Raspollini, P., Ridolfi, M., Ruhnke, R., Santee, M., Senten, C., Smale, D., Tétard, C., Urban, J., and Wood, S.: Validation of HNO_3, $ClONO_2$, and N_2O_5 from the Atmospheric Chemistry Experiment Fourier Transform Spectrometer (ACE-FTS), Atmos. Chem. Phys., 8, 3529–3562, doi:10.5194/acp-8-3529-2008, 2008.

Yokoyama, K., Sagawa, H., Manabe, T., Sato, T. O., Kuribayashi, K., Froidevaux, L., Livesey, N. J., Walker, K. A., TELIS team member, and Kasai, Y.: First observation of HCl in the upper stratosphere and mesosphere measured by Superconducting Submillimeter-Wave Limb-Emission Sounder (SMILES), J. Geophys. Res, submitted, 2013.